Available online at www.sciencedirect.com
ScienceDirect
Journal of Solid State Chemistry 180 (2007) 2298–2304
JOURNAL OF SOLID STATE CHEMISTRY
www.elsevier.com/locate/jssc

Electron-poor $SrAu_xIn_{4-x}$ ($0.5 \leqslant x \leqslant 1.2$) and $SrAu_xSn_{4-x}$ ($1.3 \leqslant x \leqslant 2.2$) phases with the $BaAl_4$-type structure

Andriy V. Tkachuk, Arthur Mar*

Department of Chemistry, University of Alberta, Edmonton, Alta., Canada T6G 2G2

Received 1 May 2007; received in revised form 5 June 2007; accepted 6 June 2007
Available online 12 June 2007

Abstract

Solid solutions $SrAu_xIn_{4-x}$ ($0.5 \leqslant x \leqslant 1.2$) and $SrAu_xSn_{4-x}$ ($1.3 \leqslant x \leqslant 2.2$) have been prepared at 700 °C and their structures characterized by powder and single-crystal X-ray diffraction. They adopt the tetragonal $BaAl_4$-type structure (space group $I4/mmm$, $Z = 2$; $SrAu_{1.1(1)}In_{2.9(1)}$, $a = 4.5841(2)$ Å, $c = 12.3725(5)$ Å; $SrAu_{1.4(1)}Sn_{2.6(1)}$, $a = 4.6447(7)$ Å, $c = 11.403(2)$ Å), with Au atoms preferentially substituting into the apical over basal sites within the anionic network. The phase width inherent in these solid solutions implies that the $BaAl_4$-type structure can be stabilized over a range of valence electron counts (vec), 13.0–11.6 for $SrAu_xIn_{4-x}$ and 14.1–11.4 for $SrAu_xSn_{4-x}$. They represent new examples of electron-poor $BaAl_4$-type compounds, which generally have a vec of 14. Band structure calculations confirm that substitution of Au, with its smaller size and fewer number of valence electrons, for In or Sn atoms enables the $BaAl_4$-type structure to be stabilized in the parent binaries $SrIn_4$ and $SrSn_4$, which adopt different structure types.
© 2007 Elsevier Inc. All rights reserved.

Keywords: Intermetallics; $BaAl_4$-type; Gold; Crystal structure; Band structure

1. Introduction

The tetragonal $BaAl_4$-type and related ordered ternary structures (such as $ThCr_2Si_2$ and $CaBe_2Ge_2$) are among the most widespread in solid-state chemistry, with several hundred examples known [1]. The electronic factors that govern their formation are well recognized [2–7]. A valence electron count (vec) of 14 electrons per formula unit, found for the vast majority of $BaAl_4$-type phases, optimizes bonding within the anionic network. However, there is now growing evidence for electron-poorer examples with a vec of 12, such as $AEZn_2Tr_2$ [7,8] $AECu_2Tt_2$ [9–11], and $AEMg_{1.7}Ga_{2.3}$ [7] (AE = alkaline earth; Tr = Al, Ga; Tt = Si, Ge). Size effects also play an important role, in the form of Madelung energy contributions involving electrostatic interactions between the cation and the anionic network. For example, although binary alkaline-earth indides $AEIn_4$ possess the optimum vec of 14, only $BaIn_4$ adopts the $BaAl_4$-type structure [12]. In contrast, $SrIn_4$ adopts a different, monoclinic $EuIn_4$-type structure [13], the $BaAl_4$-type structure being disfavoured by the small size of Sr and the large size of In [14,15]. Electron-poor $BaAl_4$-type phases can also be prepared through substitution of Au for the triel atom, as in $SrAuAl_3$ [16], $SrAuGa_3$ [17], $BaAuIn_3$ [18], and $BaAuTl_3$ [18], which have vec of 12. Because Au atoms enter the anionic network, these compounds may represent genuine examples of aurides, in which Au nominally acquires a negative oxidation state. Moreover, there is interest in $BaAuIn_3$ for use as a possible low work function cathode material in organic LEDs [19].

$SrAu_{0.5}In_{3.5}$ and $SrAuIn_3$ ($BaAl_4$-type) have been recently reported [18,20], and $SrAu_2Sn_2$ ($CaBe_2Ge_2$-type) has been briefly mentioned [3]. $SrAu_2In_2$ adopts a different (orthorhombic) structure type [20]. Given that $BaAl_4$-type compounds may be subject to nonstoichiometry, it is important to establish their phase width. We describe here structural studies on the $BaAl_4$-type solid solutions $SrAu_xIn_{4-x}$ ($0.5 \leqslant x \leqslant 1.2$) and $SrAu_xSn_{4-x}$ ($1.3 \leqslant x \leqslant 2.2$),

*Corresponding author. Fax: +1 780 492 8231.
E-mail address: arthur.mar@ualberta.ca (A. Mar).

0022-4596/$ - see front matter © 2007 Elsevier Inc. All rights reserved.
doi:10.1016/j.jssc.2007.06.004

attempting to understand their relatively wide homogeneity ranges through band structure calculations and presenting their electrical resistivity behaviour.

2. Experimental

2.1. Synthesis

Starting materials were Sr dendritic pieces (99.99%, Aldrich), Au powder (99.95%, Cerac) cold-pressed into pellets and then arc-melted into ingots, In shot (99.999%, Cerac), and Sn shot (>99.99%, Matheson). Samples of nominal composition $SrAu_xIn_{4-x}$ and $SrAu_xSn_{4-x}$ over $0<x<4$ in increments of ~0.2 were prepared. Mixtures of the elements were melted under an argon atmosphere in an Edmund Bühler MAM-1 compact arc melter. The arc-melted ingots were then placed in welded Nb containers and sealed within evacuated fused-silica tubes. After annealing at 700 °C for 10 d, the samples were quenched in cold water. Phase compositions were determined by powder X-ray diffraction (XRD) on an Inel powder diffractometer (Cu $K\alpha_1$ radiation) equipped with a CPS 120 detector and by energy-dispersive X-ray (EDX) analyses on a Hitachi S-2700 scanning electron microscope. Single-phase products with the $BaAl_4$-type structure were observed in the range $0.5\leqslant x\leqslant 1.2$ for $SrAu_xIn_{4-x}$ and $1.3\leqslant x\leqslant 2.2$ for $SrAu_xSn_{4-x}$; multiphase products were observed outside these ranges. Cell parameters refined for the $BaAl_4$-type phases obtained are listed in Table S1 (Supporting information). The arc-melted ingots were stable in air for long periods; powder samples were somewhat more sensitive, although no significant decomposition was observed over the course of the powder X-ray data collection (~12 h). Samples were handled and stored under argon atmosphere in a glove box.

The samples $SrAu_{1.1}In_{2.9}$ and $SrAu_{1.4}Sn_{2.6}$ used in the structure determination were originally obtained from direct reactions of the elements at the stoichiometry "$SrAuIn_3$" and "$SrAuSn_3$", respectively, at 950 °C for 2 d followed by cooling to room temperature over 4 d. The "$SrAuIn_3$" reaction yielded essentially phase pure $SrAu_{1.1}In_{2.9}$ (accompanied by ~2% In), but crystals of suitable size could not be obtained. The "$SrAuSn_3$" reaction yielded a multiphase sample containing small crystals of $SrAu_{1.4}Sn_{2.6}$, as well as $SrSn_3$ and Sn. The compositions of these samples correspond closely to the upper limit of Au solubility in $SrAu_xIn_{4-x}$ or the lower limit in $SrAu_xSn_{4-x}$, consistent with the stoichiometry of the reactions performed.

2.2. Structure determination

Powder XRD data for $SrAu_{1.1}In_{2.9}$ were collected on an Inel powder diffractometer and refinements were carried out with the full-profile Rietveld method using the program LHPM-Rietica [21]. Initial positions were taken from the structure of $BaAl_4$ [1]. The final cycle of least-squares refinement included scale factor, background, zero point, cell parameters, pseudo-Voigt peak profile parameters, occupancy, atomic coordinates, and isotropic displacement parameters. The fit of the Rietveld refinement results to the powder pattern is shown in Fig. 1. The results obtained here from powder data are consistent with those obtained from single-crystal data on $SrAuIn_3$ ($a = 4.5770(6)$ Å, $c = 12.371(3)$ Å; $z = 0.3909(1)$ for the mixed Au/In site) [20].

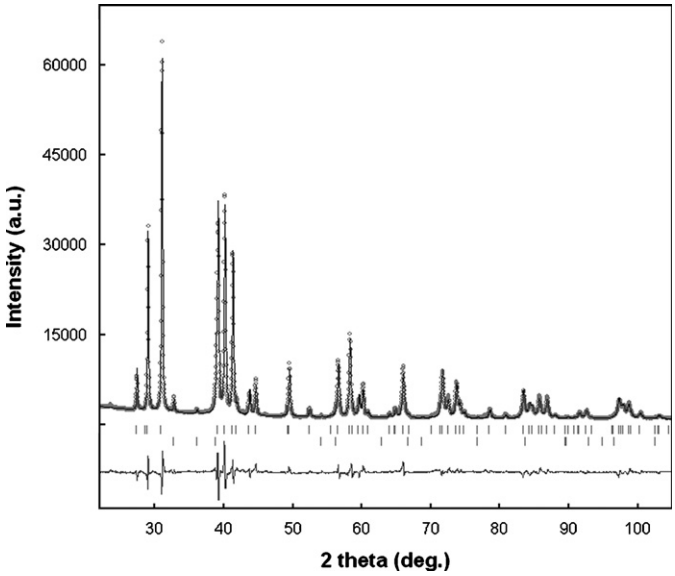

Fig. 1. Rietveld refinement results for $SrAu_{1.1}In_{2.9}$. The observed profile is indicated by circles and the calculated profile by the solid line. Bragg peak positions are located by the vertical tic marks. (The second set of tic marks corresponds to ~2% In present in this sample.) The difference plot is shown at the bottom.

Single-crystal XRD data for $SrAu_{1.4}Sn_{2.6}$ were collected on a Bruker Platform/SMART 1000 CCD diffractometer at 22 °C using ω scans. Structure solution and refinement were carried out with use of the SHELXTL (version 6.12) program package [22]. Face-indexed numerical absorption corrections were applied. Structure solution and refinement proceeded in a straightforward manner. Further data, in CIF format, have been sent to Fachinformationszentrum Karlsruhe, Abt. PROKA, 76344 Eggenstein-Leopoldshafen, Germany, as Supplementary material no. CSD-418165 and can be obtained by contacting FIZ (quoting the article details and the corresponding CSD numbers).

Crystal data and further details of the data collection for $SrAu_{1.1}In_{2.9}$ and $SrAu_{1.4}Sn_{2.6}$ are given in Table 1. Final values of the positional and displacement parameters are given in Table 2. Selected interatomic distances are listed in Table 3.

2.3. Band structure

Tight-binding linear muffin tin orbital (TB-LMTO) band structure calculations were performed within the local density and atomic spheres approximations using the

Table 1
Crystallographic data for $SrAu_{1.1}In_{2.9}$ and $SrAu_{1.4}Sn_{2.6}$

Formula	$SrAu_{1.1(1)}In_{2.9(1)}$	$SrAu_{1.4(1)}Sn_{2.6(1)}$
Formula mass (amu)	636.23	668.05
Space group	*I*4/*mmm* (no. 139)	*I*4/*mmm* (no. 139)
a (Å)	4.5841(2)	4.6447(7)
c (Å)	12.3725(5)	11.403(2)
V (Å^3)	260.00(2)	246.0(1)
Z	2	2
ρ_{calcd} (g cm^{-3})	8.123	9.019
Radiation	Cu Kα_1, $\lambda = 1.54056$ Å	Mo Kα, $\lambda = 0.71073$ Å
μ (mm^{-1})	169.9	64.0
2θ range	15.0–110.0°	7.1–60.9°
No. of data collected	3276 data points	1470 ($R_{int} = 0.043$)
No. of unique data	66 Bragg reflections	139 (125 with $F^2 > 2\sigma(F^2)$)
No. of variables	20	12
Residuals[a]	$R_B = 0.034$, $R_p = 0.067$, $R_{wp} = 0.084$	$R(F)$ ($F^2 > 2\sigma(F^2)$) $= 0.038$, $R_w(F^2) = 0.096$

[a] $R_B = \sum |I_o - I_c| / \sum I_o$, $R_p = \sum |y_o - y_c| / \sum y_o$, $R_{wp} = [\sum [w(y_o - y_c)] / \sum w y_o^2]^{1/2}$, $R(F) = \sum ||F_o| - |F_c|| / \sum |F_o|$, $R_w(F_o^2) = [\sum [w(F_o^2 - F_c^2)^2] / \sum w F_o^4]^{1/2}$, $w^{-1} = [\sigma^2(F_o^2) + (Ap)^2 + Bp]$ where $p = [\max(F_o^2, 0) + 2F_c^2]/3$.

Table 2
Atomic coordinates and equivalent isotropic displacement parameters for $SrAu_{1.1}In_{2.9}$ and $SrAu_{1.4}Sn_{2.6}$

Atom	Wyckoff position	Occupancy	*x*	*y*	*z*	U_{iso} or U_{eq} (Å^2)[a]
$SrAu_{1.1}In_{2.9}$						
Sr	2*a*	1	0	0	0	0.0129(11)
In1	4*d*	1	0	1/2	1/4	0.0076(8)
Au2/In2	4*e*	0.53(2)/0.47(2)	0	0	0.3911(1)	0.0068(6)
$SrAu_{1.4}Sn_{2.6}$						
Sr	2*a*	1	0	0	0	0.0273(12)
Au1/Sn1	4*d*	0.28(4)/0.72(4)	0	1/2	1/4	0.0284(6)
Au2/Sn2	4*e*	0.40(4)/0.60(5)	0	0	0.3863(1)	0.0310(6)

[a] U_{iso} applies to $SrAu_{1.1}In_{2.9}$ and U_{eq} to $SrAu_{1.4}Sn_{2.6}$. U_{eq} is defined as one-third of the trace of the orthogonalized U_{ij} tensor.

Table 3
Selected interatomic distances (Å) in $SrAu_{1.1}In_{2.9}$ and $SrAu_{1.4}Sn_{2.6}$[a]

	$SrAu_{1.1}In_{2.9}$	$SrAu_{1.4}Sn_{2.6}$
Sr–*X*2 ($\times 8$)	3.5102(5)	3.5310(7)
Sr–*X*1 ($\times 8$)	3.8498(1)	3.6769(4)
*X*1–*X*2 ($\times 4$)	2.8814(8)	2.7943(10)
*X*1–*X*1 ($\times 4$)	3.2414(1)	3.2843(2)
*X*2–*X*2	2.694(3)	2.593(3)

[a] Disordered sites *X*1 and *X*2 contain a mixture of Au with In or Sn atoms.

Stuttgart TB-LMTO program [23]. The basis sets consisted of Sr 5*s*, 5*p*, 4*d*, 4*f*; Au 6*s*, 6*p*, 5*d*, 5*f*; and In or Sn 5*s*, 5*p*, 5*d*, 4*f* orbitals, with the Sr 5*p*, 4*f*; Au 4*f*; and In or Sn 5*d*, 4*f* orbitals being downfolded. Band structures of $SrAuIn_3$ and $SrAu_2Sn_2$ with hypothetical ordered $BaNiSn_3$-type (space group *I*4*mm*) and $CaBe_2Ge_2$-type (space group *P*4/*nmm*) structures were calculated to model $SrAu_{1.1}In_{2.9}$ and $SrAu_{1.4}Sn_{2.6}$, respectively. Integrations in reciprocal space were carried out with an improved tetrahedron method over 756 independent *k* points within the first Brillouin zone for $SrAuIn_3$ ($BaNiSn_3$-type) and 180 *k* points for $SrAu_2Sn_2$ ($CaBe_2Ge_2$-type).

2.4. Electrical resistivity

Electrical resistivities on a fragment of a $SrAu_{1.1}In_{2.9}$ ingot and on a single crystal of $SrAu_{1.4}Sn_{2.6}$ were measured by standard four-probe techniques on a Quantum Design PPMS system equipped with an ac transport controller (Model 7100). The current was 100 μA and the frequency was 16 Hz.

3. Results and discussion

$SrAu_xIn_{4-x}$ and $SrAu_xSn_{4-x}$ solid solutions with the $BaAl_4$-type structure have been prepared, with their limits of solid solubility assessed by identifying the composition regions where single-phase product was present from arc-melting reactions. Fig. 2 shows plots of the cell parameters, which contract with greater substitution of smaller Au atoms for In or Sn. The degree of Au substitution in $SrAu_xIn_{4-x}$ ($0.5 \leqslant x \leqslant 1.2$) is modest, in good agreement with that recently reported ($0.5 \leqslant x \leqslant 1.0$) by Dai and

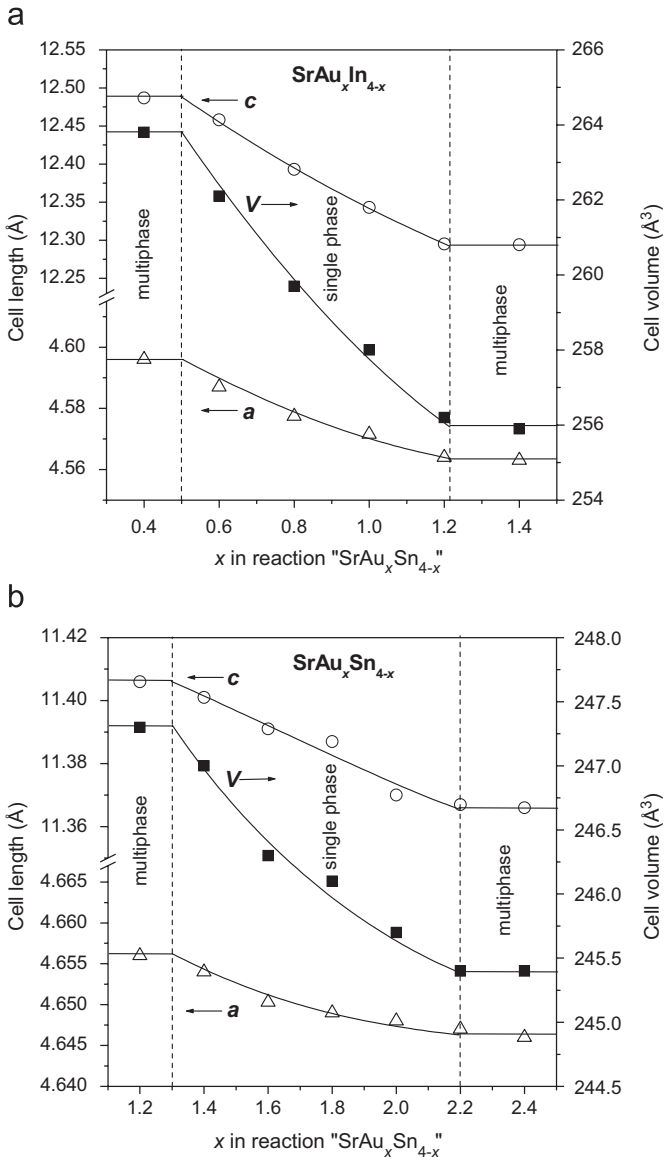

Fig. 2. Plot of cell parameters vs. x for $BaAl_4$-type phase observed in reactions with nominal composition of (a) $SrAu_xIn_{4-x}$ or (b) $SrAu_xSn_{4-x}$.

Corbett, who use slightly different synthetic conditions [20]. At larger values of x in the $SrAu_xIn_{4-x}$ system, other phases appear, including a $SrAu_2In_2$ compound adopting a different structure ($BaAu_2In_2$-type) [20]. In contrast, Au substitution is more significant in $SrAu_xSn_{4-x}$ ($1.3 \leqslant x \leqslant 2.2$), accompanied by a drastic reduction in cell volume. The different substitutional ranges found in $SrAu_xIn_{4-x}$ and $SrAu_xSn_{4-x}$ imply an influence of electron count. Moreover, the c/a ratio decreases from ~2.7 for $SrAu_xIn_{4-x}$ to ~2.5 for $SrAu_xSn_{4-x}$, reflecting bond strengthening along the c direction. Although the substitution of Au for triel atoms to stabilize the $BaAl_4$-type structure in binary $AETr_4$ (Tr = Al, Ga, In, Tl) phases is now well recognized [16–18,24], there appear to be no previous examples of the analogous effect of Au substitution for Sn. Other known phases in the Sr–Au–(In or Sn) systems are $Sr_2Au_3In_4$ [25], SrAuSn [26], and $SrAuSn_2$ [27].

There is a recent example of gallium–tin mixing in $BaGa_{4-x}Sn_x$ ($x = 0.89(2)$) with the $BaAl_4$-type structure [28]. Indeed, no binary phases of the form $AESn_4$ have been found except for the superconducting compound $SrSn_4$, which adopts a different (orthorhombic) structure [29]. The $SrAu_xSn_{4-x}$ solid solution thus represents a new example of Au stabilization of the $BaAl_4$-type structure in an alkaline-earth stannide.

The $BaAl_4$-type structure adopted by $SrAu_xIn_{4-x}$ ($0.5 \leqslant x \leqslant 1.2$) and $SrAu_xSn_{4-x}$ ($1.3 \leqslant x \leqslant 2.2$) consists of Sr cations occupying cages within a three-dimensional anionic network of $X1$ and $X2$ atoms stacked in square nets (Fig. 3). Each $X1$ atom is surrounded by four $X2$ atoms tetrahedrally and by four $X1$ atoms in a square plane, whereas each $X2$ atom is surrounded by four $X1$ and one $X2$ atoms in a square pyramid. Often, $X1$ are referred to as the basal atoms and $X2$ as the apical atoms [4,7]. Two apical atoms are linked to form an $X2$–$X2$ pair, whose highly variable bond length is a characteristic feature of this structure type. Structural determinations reveal that in $SrAu_{1.1}In_{2.9}$, the basal sites are occupied exclusively by In atoms and the apical sites by a mixture of roughly equal proportions of Au and In atoms. In contrast, in $SrAu_{1.4}Sn_{2.6}$, both sites are disordered, with the basal sites

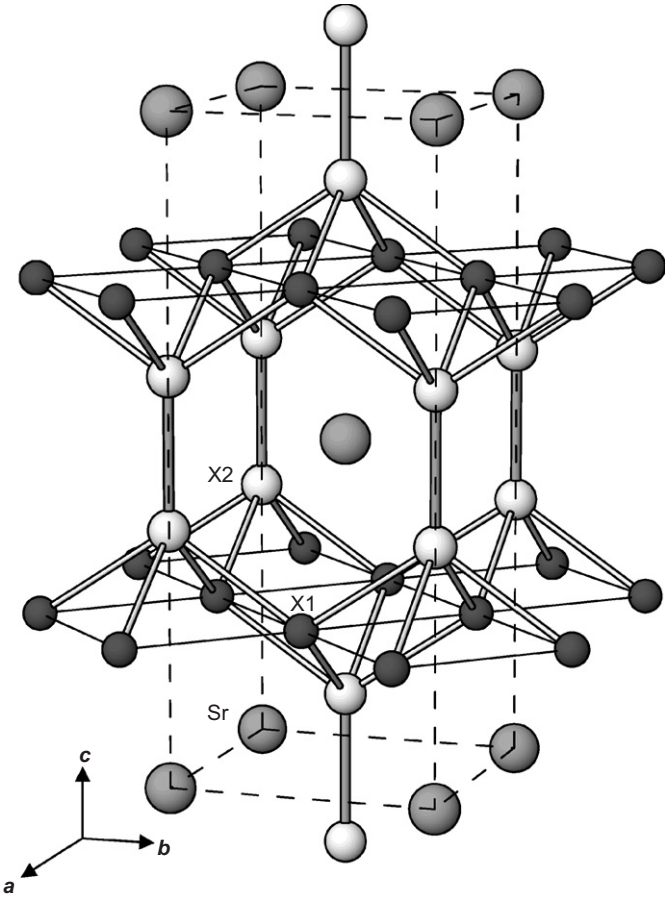

Fig. 3. $BaAl_4$-type structure of $SrAu_xIn_{4-x}$ or $SrAu_xSn_{4-x}$. Disordered sites $X1$ and $X2$ contain a mixture of Au with In or Sn atoms.

containing less Au (0.28(4) Au, 0.72(4) Sn) than the apical sites (0.40(4) Au, 0.60(5) Sn).

The absence of a $BaAl_4$-type structure of $SrIn_4$ has been previously attributed to the ineffective bonding of Sr atoms within its coordination polyhedron arising from a size mismatch [13–15]. A computational structure optimization of $SrIn_4$ ($BaAl_4$-type) gave relatively long distances from Sr to its coordinating atoms (3.77, 3.94 Å) [14]. In $SrAu_{1.1}In_{2.9}$, these distances have been reduced to more reasonable values (Sr–In1, 3.5102(5) Å; Sr–Au2/In2, 3.8498(1) Å). On going from the $SrAu_xIn_{4-x}$ to the $SrAu_xSn_{4-x}$ phases, a significant contraction in the cell parameters has been noted above. The source of the contraction along *c* lies primarily in the shortening of Sr–*X*1 and *X*2–*X*2 bonds (Table 3). The distance within the *X*2–*X*2 pair in $SrAu_{1.4}Sn_{2.6}$ is remarkably short (2.593(3) Å), compared to other Au-substituted $BaAl_4$-type phases [16–18] or to any combination of the Pauling single-bond metallic radii (Au, 1.34 Å; Sn, 1.42 Å) [30].

To understand some of the observations noted above, electronic band structures were calculated. To model $SrAu_{1.1}In_{2.9}$, a hypothetically ordered structure ($BaNiSn_3$-type) was examined, in which the basal atoms are all In (as in the observed structure) but the apical atoms are arranged in ordered 2.694 Å Au–In pairs. The DOS and COHP curves are shown in Fig. 4a. In the band structure of hypothetical $SrIn_4$ ($BaAl_4$-type) with a vec of 14, the Fermi level falls exactly at a prominent pseudogap where

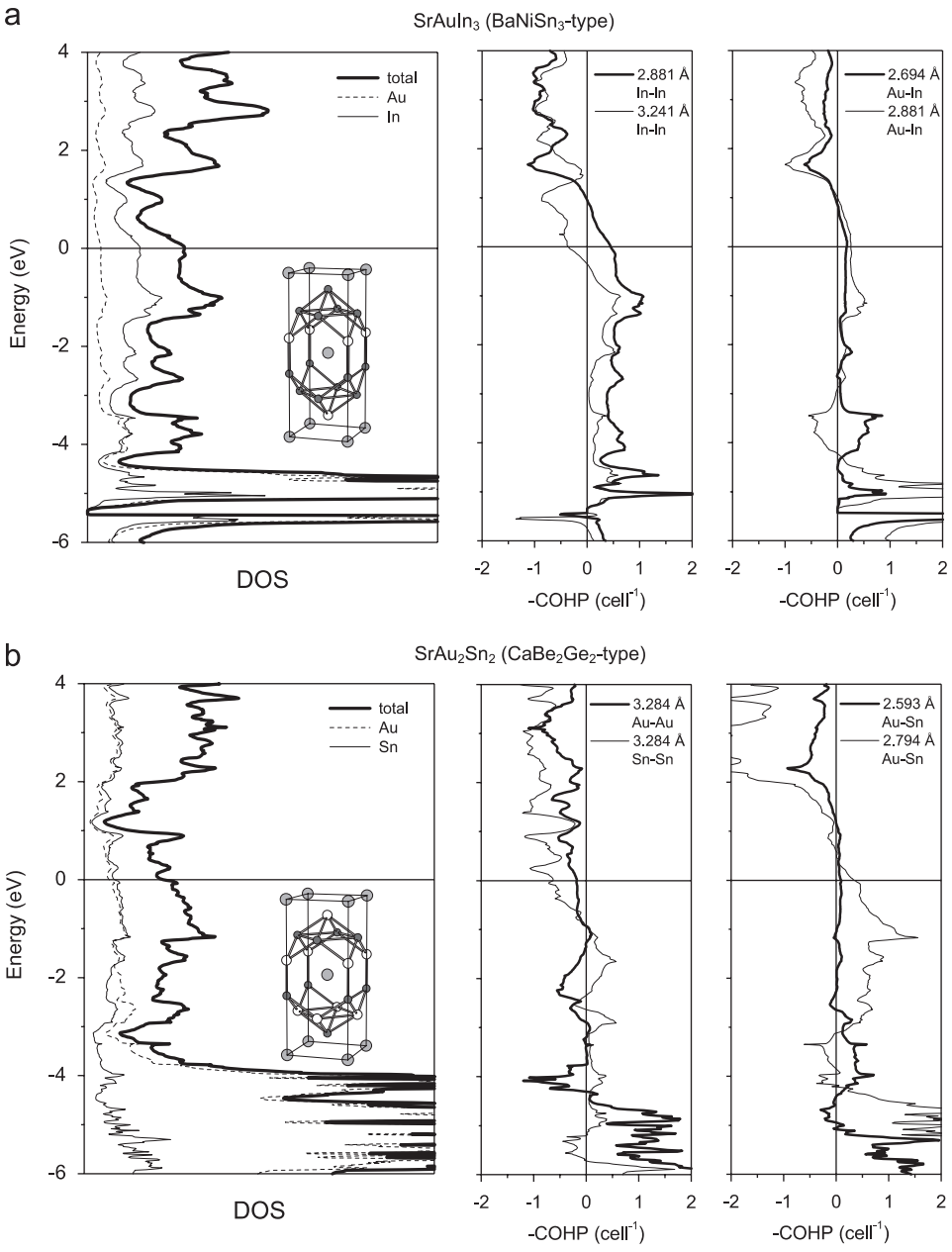

Fig. 4. Density of states (DOS) and crystal orbital Hamilton population (COHP) curves for hypothetical ordered structures of (a) $SrAuIn_3$ ($BaNiSn_3$-type) and (b) $SrAu_2Sn_2$ ($CaBe_2Ge_2$-type). The Fermi level is marked by a horizontal line at 0 eV.

In–In bonding is optimized [14]. At a lower vec of 12, the Fermi level in $SrAuIn_3$ falls below what would correspond to this gap (near 1.3 eV), which is also not very pronounced. Inspection of the COHP curves reveals that most, but not all, of the Au–In and In–In bonding states are filled. Most of the heteroatomic Au–In bonding stabilization is provided from levels below −3 eV, whereas In–In bonding remains sensitive to variations in electron count near the Fermi level. In particular, the gain in apical-basal In–In bonding (2.881 Å) that would ensue from addition of more electrons to the system is offset by the loss in basal–basal In–In bonding (3.241 Å), the turning point being at 1.3 eV (vec of 14). The range of solid solubility observed in $SrAu_xIn_{4-x}$ ($0.5 \leqslant x \leqslant 1.2$) corresponds to a relatively constant bonding energy as the vec varies between 13.0 and 11.6.

The electronic structure of $SrAu_{1.4}Sn_{2.6}$ can be modeled by several possibilities. With a greater Au content and Au/Sn disorder occurring in both apical and basal sites, the likelihood for homoatomic Au–Au bonds must be considered. This can be modeled by taking "$SrAu_2Sn_2$" with a $ThCr_2Si_2$-type structure. Comparison of total energies shows that placing Au atoms in the apical sites (forming short 2.593 Å Au–Au bonds within apical-apical pairs) is more stable than placing them in the basal sites (forming long 3.284 Å Au–Au contacts within the square nets) by 0.18 eV/f.u. This small "colouring energy" agrees well with the critical value (~0.2–0.4 eV/f.u.) at which disorder of the apical and basal sites is predicted to occur in ternary phases with the $BaAl_4$-type structure [7]. The crystal structure of $SrAu_{1.4}Sn_{2.6}$ also shows that the apical sites are Au-richer than the basal sites, consistent with their well-understood preference to be occupied by the more electronegative atoms [4]. Interestingly, instead of a $ThCr_2Si_2$-type structure (with apical Au), the $CaBe_2Ge_2$-type structure is even more stable, by 0.27 eV/f.u. In this structure, Au and Sn atoms alternately occupy the apical and basal sites in an ordered manner, so that the 2.593 Å apical-apical pairs are treated as heteroatomic Au–Sn bonds. The DOS and COHP curves for this model are shown in Fig. 4b. The short apical–apical Au–Sn bond is rather strong, as confirmed by its integrated COHP of 2.7 eV/bond, and results from occupation of bonding levels deep in energy (below −2 eV). Because Sn has more valence electrons than In, Au substitution should occur to a greater degree in $SrAu_xSn_{4-x}$ than in $SrAu_xIn_{4-x}$ to maintain a reasonable vec; as observed, the solid solution range ($1.3 \leqslant x \leqslant 2.2$) corresponds to a vec of 14.1–11.4. The pseudogap above the Fermi level (near 1 eV) is quite distinct and the band structure shows clearly that antibonding Au–Au and Sn–Sn states would have to be occupied if the number of electrons is increased above that for $SrAu_2Sn_2$ (vec of 12). The instability of $SrSn_4$ with a $BaAl_4$-type structure, with an even greater number of electrons, is also related to the occupation of antibonding Au–Sn levels. The arguments invoked previously relating the insensitivity of vec to bonding energy within the $SrAu_xSn_{4-x}$ solid solution do not seem to apply here as convincingly. However, it is important to remember that the size requirements of the Sr cation must also be fulfilled. With a greater substitution of Au, the contraction of the structure allows better size matching of the Sr cations within their coordination polyhedra, as seen in the shorter Sr–*X*1 distances (3.5310(7) Å, 3.6769(4) Å).

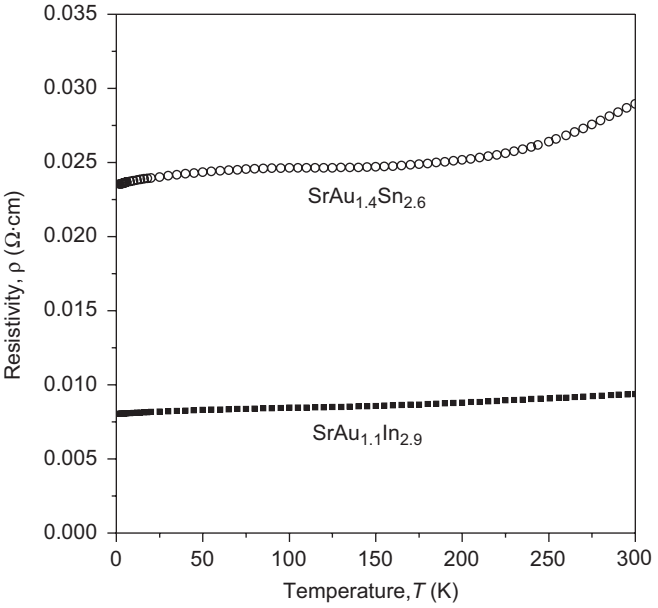

Fig. 5. Electrical resistivity of $SrAu_{1.1}In_{2.9}$ and $SrAu_{1.4}Sn_{2.6}$.

With no gap at the Fermi level, it is expected that these compounds should behave as metallic conductors. Electrical resistivity curves for $SrAu_{1.1}In_{2.9}$ and $SrAu_{1.4}Sn_{2.6}$ are shown in Fig. 5. Although the resistivity does decrease with lower temperatures, the absolute values are high ($\rho_{300K} = 1.0 \times 10^{-2}\,\Omega\,cm$ for $SrAu_{1.1}In_{2.9}$ and $2.9 \times 10^{-2}\,\Omega\,cm$ for $SrAu_{1.4}Sn_{2.6}$) and the temperature dependence is very weak, consistent with the high degree of disorder in these materials.

Acknowledgments

The Natural Sciences and Engineering Research Council of Canada and the University of Alberta supported this work. We thank Dr. Robert McDonald and Dr. Michael J. Ferguson (X-ray Crystallography Laboratory) for the X-ray data collection and Ms. Christina Barker (Department of Chemical and Materials Engineering) for assistance with the EDX analysis.

Appendix A. Supplementary data

Supplementary data associated with this article can be found in the online version at doi:10.1016/j.jssc.2007.06.004.

References

[1] W.B. Pearson, J. Solid State Chem. 56 (1985) 278–287.
[2] R. Hoffmann, C. Zheng, J. Phys. Chem. 89 (1985) 4175–4181.
[3] C. Zheng, R. Hoffmann, J. Am. Chem. Soc. 108 (1986) 3078–3088.

[4] C. Zheng, R. Hoffmann, Z. Naturforsch. 41B (1986) 292–320.
[5] J.K. Burdett, G.J. Miller, Chem. Mater. 2 (1990) 12–26.
[6] C. Zheng, J. Am. Chem. Soc. 115 (1993) 1047–1051.
[7] U. Häussermann, S. Amerioun, L. Eriksson, C.-S. Lee, G.J. Miller, J. Am. Chem. Soc. 124 (2002) 4371–4383.
[8] G. Cordier, E. Czech, H. Schäfer, Z. Naturforsch. 39B (1984) 1629–1632.
[9] W. Rieger, E. Parthé, Monatsh. Chem. 100 (1969) 444–454.
[10] B. Eisenmann, N. May, W. Müller, H. Schäfer, A. Weiss, J. Winter, G. Ziegleder, Z. Naturforsch. 25B (1970) 1350–1352.
[11] W. Dörrscheidt, N. Niess, H. Schäfer, Z. Naturforsch. 31B (1976) 890–891.
[12] M. Wendorff, C. Röhr, Z. Anorg. Allg. Chem. 631 (2005) 338–349.
[13] D.-K. Seo, J.D. Corbett, J. Am. Chem. Soc. 122 (2000) 9621–9627.
[14] S. Amerioun, U. Häussermann, Inorg. Chem. 42 (2003) 7782–7788.
[15] J.-G. Mao, A.M. Guloy, J. Alloys Compd. 363 (2004) 143–149.
[16] F. Hulliger, J. Alloys Compd. 218 (1995) 255–258.
[17] G. Cordier, T. Friedrich, Z. Kristallogr. 201 (1992) 310–311.
[18] S. Liu, J.D. Corbett, Inorg. Chem. 43 (2004) 4988–4993.
[19] M.A. Uijttewaal, G.A. de Wijs, R.A. de Groot, Surf. Sci. 600 (2006) 2495–2500.
[20] J.-C. Dai, J.D. Corbett, Inorg. Chem. 46 (2007) 4592–4598.
[21] B. Hunter, LHPM-Rietica, version 1.7.7, International Union of Crystallography Commission on Powder Diffraction Newsletter, no. 20 (summer), 1998, ⟨www.rietica.org⟩.
[22] G.M. Sheldrick, SHELXTL, version 6.12, Bruker AXS Inc., Madison, WI, 2001.
[23] R. Tank, O. Jepsen, A. Burkhardt, O.K. Andersen, TB-LMTO-ASA Program, Version 4.7, Max Planck Institut für Festkörperforschung, Stuttgart, 1998.
[24] Yu. Grin, M. Ellner, B. Predel, G. Cordier, J. Alloys Compd. 216 (1994) 207–211.
[25] R.-D. Hoffmann, R. Pöttgen, C. Rosenhahn, B.D. Mosel, B. Künnen, G. Kotzyba, J. Solid State Chem. 145 (1999) 283–290.
[26] R.-D. Hoffmann, R. Pöttgen, D. Kussmann, D. Niepmann, H. Trill, B.D. Mosel, Solid State Sci. 4 (2002) 481–487.
[27] S. Esmailzadeh, R.-D. Hoffmann, R. Pöttgen, Z. Naturforsch. 59B (2004) 1451–1457.
[28] P.H. Tobash, Y. Yamasaki, S. Bobev, Acta Crystallogr. E 63 (2007) i35–i37.
[29] S. Hoffmann, T.F. Fässler, Inorg. Chem. 42 (2003) 8748–8754.
[30] L. Pauling, The Nature of the Chemical Bond, third ed., Cornell University Press, Ithaca, NY, 1960.